AIP | Applied Physics Letters

Development of a fast electromagnetic beam blanker for compressed sensing in scanning transmission electron microscopy

A. Béché, B. Goris, B. Freitag, and J. Verbeeck

Citation: Applied Physics Letters **108**, 093103 (2016); doi: 10.1063/1.4943086
View online: http://dx.doi.org/10.1063/1.4943086
View Table of Contents: http://scitation.aip.org/content/aip/journal/apl/108/9?ver=pdfcov
Published by the AIP Publishing

Development of a fast electromagnetic beam blanker for compressed sensing in scanning transmission electron microscopy

A. Béché,[1,a)] B. Goris,[1] B. Freitag,[2] and J. Verbeeck[1]
[1]EMAT, University of Antwerp, Groenenborgerlaan 171, 2020 Antwerp, Belgium
[2]FEI Electron Optics, Achtseweg Noord 5, 5651 GG Eindhoven, The Netherlands

(Received 26 November 2015; accepted 19 February 2016; published online 1 March 2016)

The concept of compressed sensing was recently proposed to significantly reduce the electron dose in scanning transmission electron microscopy (STEM) while still maintaining the main features in the image. Here, an experimental setup based on an electromagnetic beam blanker placed in the condenser plane of a STEM is proposed. The beam blanker deflects the beam with a random pattern, while the scanning coils are moving the beam in the usual scan pattern. Experimental images at both the medium scale and high resolution are acquired and reconstructed based on a discrete cosine algorithm. The obtained results confirm that compressed sensing is highly attractive to limit beam damage in experimental STEM even though some remaining artifacts need to be resolved. © *2016 AIP Publishing LLC*. [http://dx.doi.org/10.1063/1.4943086]

One of the most challenging topics in modern transmission electron microscopy (TEM) is to perform experiments on soft materials as they suffer from irradiation damage that can range from structural modification to the complete destruction of the sample. Such sample modifications are even more problematic when 3D and/or analytical characterizations are involved. In order to overcome this issue, a wide range of different approaches are being tested in the TEM community, such as the reduction in the kinetic energy of the fast electrons,[1–3] improving the detection efficiency of cameras,[4–7] time resolved approaches,[8–10] and many more. Relatively recently, the concept of compressed sensing was proposed to significantly reduce the electron dose while maintaining all the important features in Scanning TEM (STEM) image.[11–14] Compressed sensing is based on the assumption that images are not a random succession of pixel values and present some structure. The condition for a proper image reconstruction is that the original image has a sparse representation in a specific basis, which can be chosen prior to image reconstruction.[15–17] Therefore, the image can be approximated from a small subset of pixels randomly taken from the completely sampled image. Depending on the sparsity, such reconstructed image can be very close to the fully sampled image while considerably reducing the required dose. The process is somewhat comparable to image compression algorithms, e.g., in the jpeg format, that try to represent images with reduced storage space by exploiting the structure present in a typical image.

Over the last few years, some studies have proposed to apply compressed sensing to transmission electron microscopy images using different types of reconstruction algorithms based on the Bayesian dictionary learning technique,[12] wavelet frame based,[13] or total variation inpainting.[14] All of this work was done on virtually masked images starting from a fully sampled experimental or stored image and applying a digital mask to it, taking out a number of randomly selected pixels. This indeed has shown a great potential for compressed sensing in STEM but should be seen as an idealized simulation, assuming that experimental random pixel measurements would be possible. Implementing compressed sensing in practice is complicated by the fact that typical scan engines in STEM microscopes are not designed to be driven in a non-regular pattern as would be required. An alternative is to make use of a beam blanker that can switch the electron beam on and off while keeping the conventional regular scanning pattern. In this paper, we present the experimental realization of such a beam blanker based on electromagnetic deflection and demonstrate that we obtain experimental compressed sensing in a STEM in both medium and high resolution (HR). By blanking the beam using a pseudorandom generator,[18] it was possible to acquire images with a limited number of pixels and reconstruct them using the discrete cosine transform.[23,24] This demonstrates that compressed sensing is an experimentally viable technique in STEM, opening up the predicted advantages of the technique for experimental research.

The aim in compressed sensing acquisition is to illuminate only parts of the sample. Scanning imaging modes are especially well suited for this operation as images are acquired in a pixel by pixel way. Generally, one of the two following strategies can be implemented to achieve compressed sensing in such mode: (i) blanking the beam in between two illuminated pixels or (ii) driving the scanning coils in a specific way to jump from one pixel to a non-adjacent next pixel. Anderson *et al.*[19] achieved successful acquisitions with the second strategy in an SEM. Doing this in a STEM is more complicated due to the higher beam location precision and stronger magnetic field that is required to deflect faster electrons. The blanking method, although offering less gain in terms of acquisition time, has the distinct advantage of a simpler hardware setup and will allow us to test compressed sensing in STEM.

In a (S)TEM, the pre-specimen beam blanker is located at the gun level but suffers from a relatively slow response time, making it unattractive for the current purpose of blanking the beam during scanning. Our main challenge was then

a)Author to whom correspondence should be addressed. Electronic mail: armand.beche@uantwerpen.be

to realize a sufficiently fast beam blanker compatible with a typical microsecond range dwell times in STEM. At first, we redesigned the complete condenser (C2) aperture holder with four electrical feedthrough contacts. A picture of the custom built holder is displayed in Figure 1 showing the four aperture slots together with four electrical contacts. Two of these contacts power the solenoid, the two others being left for future uses. We deflect the electron beam making use of a simple solenoid wrapped around the first condenser aperture. The solenoid produces a quasi-homogeneous magnetic field at the plane of the aperture, which deflects the electrons due to the Lorentz force. At the given winding density, it turns out that a current of 250 mA is capable of deflecting a 300 keV focused probe about 350 nm away from the sample area. A selected area (SA) aperture was introduced into the path of the beam to prevent high angle diffraction signal from reaching the detector when the beam blanker was deflecting the beam. The solenoid has a series resistance of $R_s = 0.75\ \Omega$, a self-inductance of $L_s = 5\ \mu$H, and an estimated capacitance of $C_s = 12$ pF.[20,21] These parameters set the maximum switching speed, which can be estimated as $\tau = \sqrt{(L_s C_s)} \simeq 8$ ns, much shorter than typical STEM dwell times.

An Arduino[22] microcontroller unit linked to a switched current source was used to drive the deflector coil synchronized with the STEM scan engine. The microcontroller was then programmed to activate or not the fast beam blanker based on a (pseudo) random[18] generator. A pixel will be illuminated if the random generator with uniform probability distribution between 1 and 100 draws a number higher than X, with X the percentage of blanked pixels over the whole scan. Figure 2 displays a schematic of our experimental setup.

In order to correctly reconstruct the acquired sparsely sampled image, the reconstruction algorithm needs to have access to the acquisition mask, namely, knowing when the beam was blanked or unblanked. As the storage space on the microcontroller was limited, we used a workaround to obtain the random mask by acquiring a zero loss (ZL) EELS map together with the High Angle Annular Dark Field (HAADF) STEM image. In order to obtain a ZL peak of sufficient intensity, the single pixel exposure time was set to 0.5 ms. Even though this value is unreasonably high compared to typical dwell times used in STEM, it nevertheless allows us

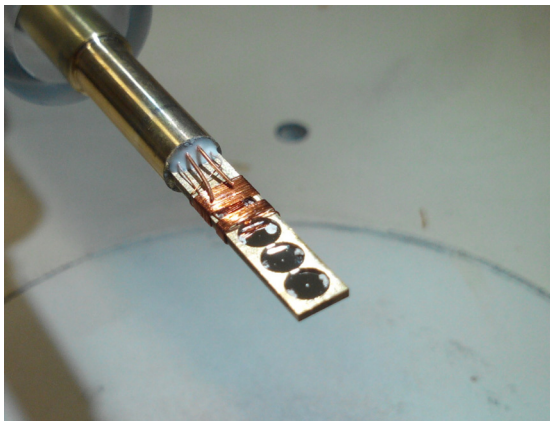

FIG. 1. C2 electric contact aperture holder mounted with a solenoid. Extreme left and right contacts power the solenoid.

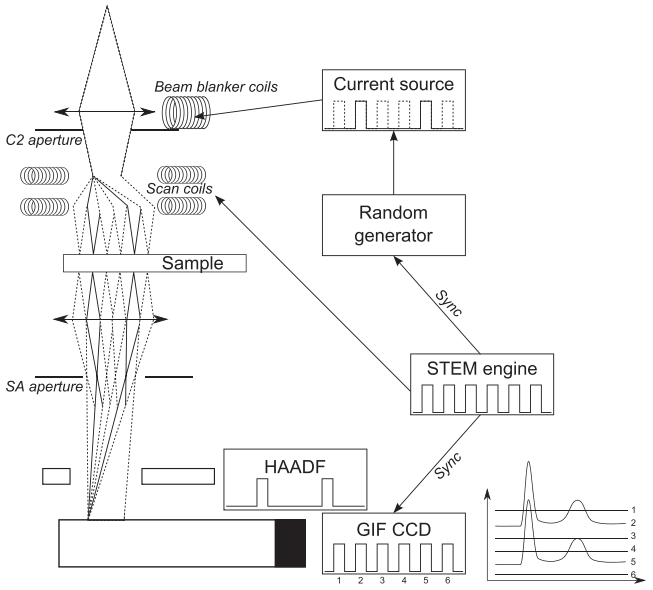

FIG. 2. Schematic of the compressed sensing acquisition setup. The STEM engine drives the STEM coils and synchronized the GIF CCD and the random generator. Depending on the random number generator, the beam is either blanked (dashed trajectory) or not, leading to the absence or presence of signal on the HAADF detector and zero loss peak in the EELS map.

to prove the setup works and to verify the efficiency of beam blanking. In a later stage, the described workaround will disappear and the dwell time will be only limited by the maximum speed at which the beam blanker can be driven, which should comfortably be in the microsecond to nanosecond range. In order to reconstruct the images from the subsampled projections, an in-painting step is required to fill the missing pixels in the images, which corresponds to solving the following equations:

$$\hat{x} = argmin_x \| \Phi x - b \|_{\ell 2}^2 \text{ with } \| \Psi_x \|_{\ell 1} < \lambda, \qquad (1)$$

where $\hat{x}$ corresponds to the estimated reconstruction of image x, b equals the measured pixels, and Φ is a subsampling operator that selects the imaged pixels. The operator Ψ represents the sparsifying transform that can be chosen prior to the reconstruction, $\| \ \|_{lp}$ is the ℓ-norm of order p, and λ is a parameter that can be adjusted according to the sparsity of the image after the sparsifying transform. In this work, a discrete cosine transform is selected, which is well suited for images showing a local periodicity such as high resolution STEM projections. The reconstruction is implemented in Matlab using the spgl1 algorithm.[23,24] More elaborate transforms can easily be implemented but we focused here on the experimental realization of the fast beam blanker.

The effect of compressed sensing on STEM image acquisition and reconstruction was investigated using two samples with rather different properties. First, medium resolution STEM imaging was investigated on a standard gold cross grating sample (Pelco #607). This sample has the advantage of presenting a very high density of gold nanoparticles with quite complex agglomerated shapes. Second, HRSTEM was investigated on a complex perovskite oxide sample consisting of an orthorhombic [110] $NbGaO_3$ substrate covered with 6 atomic layers of $SrTiO_3$ and a 10 nm of $LaSrMnO_3$.[25] In the [1–10] observation direction, the lattice parameter is well above the

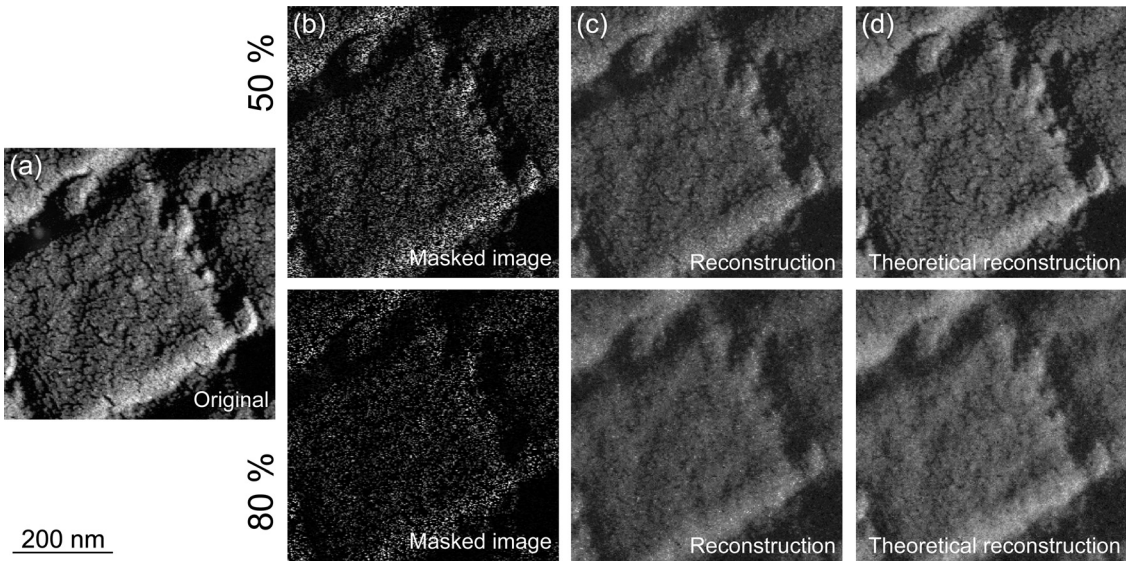

FIG. 3. Experimental acquisition of STEM images at medium scale: (a) original image, (b) images acquired at random positions with either 50% or 80% of beam blanking, (c) reconstructed images, and (d) reconstructed images from a masked original image.

theoretical resolution limit of our instrument, thus ensuring optimal conditions for the image reconstruction. Both samples also have the advantage of being relatively beam hard, allowing for the extra acquisition time needed for the ZL spectrum mapping workaround. One could argue that both samples are rather far from the beam sensitive samples one would expect when discussing compressed sensing; however, they allow us to study the feasibility of this imaging technique without beam damage issues complicating the interpretation of the results.

Both samples were imaged with three different acquisition schemes: no blanking, 50% and 80% of beam blanking. The total dose is then effectively reduced by a factor of 2 and 5. The total frame size was set to 256×256 pixels with a dwell time of 0.5 ms in standard HRSTEM illumination conditions, with an acceleration voltage of 300 kV, a convergence angle of 20 mrad with a beam current of 50 pA using a 20 μm C2 aperture. The simultaneous ZL EELS map was acquired with a collection angle of 35 mrad using a dispersion of 0.25 eV/pixel and a 5 mm GIF entrance aperture.

The experimental images on the cross grating sample are grouped in Figure 3 together with their reconstructions based on the discrete cosine algorithm. For the 50% blanked case, the main features of the image are retrieved in the reconstructed image, even though the resolution decreased somewhat. The 80% blanked image reveals a lack of details and only the larger image features are reconstructed while the finer structural details are lost. Note that in terms of redundancy, the cross grating is a very challenging case for compressed sensing for the same reasons that this is an excellent sample to align an electron microscope as it provides irregular features without favoring certain directions over others. For the HRSTEM sample displayed in Figure 4, both 50% and 80% blanking cases are still revealing

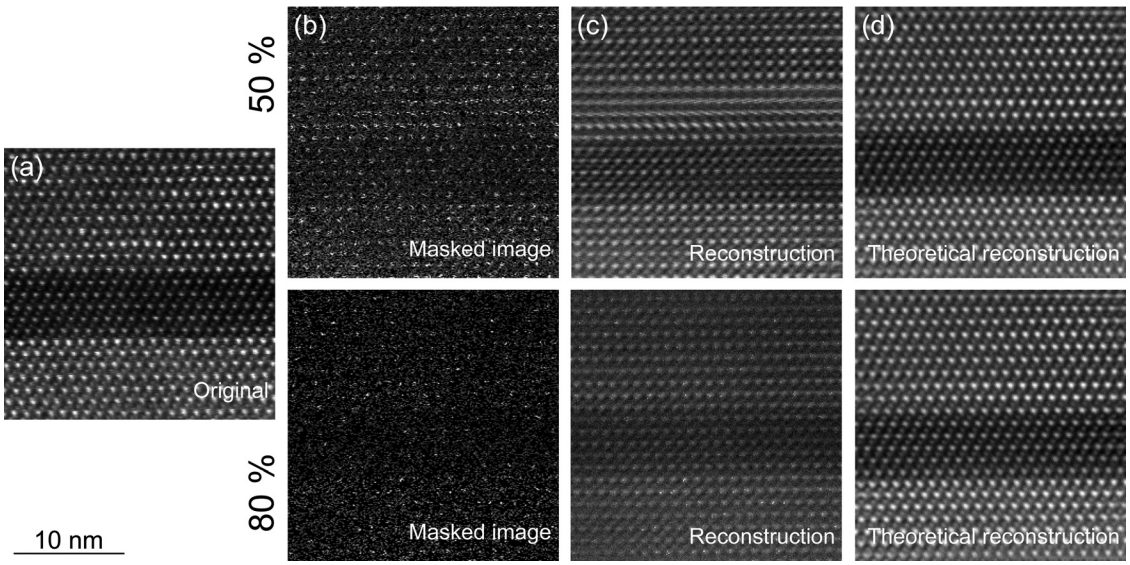

FIG. 4. Experimental acquisition of STEM images at atomic scale: (a) original unblanked, (b) images with either 50% or 80% of pixels blanked, (c) reconstructed images, and (d) reconstructed images from a masked original image.

acceptable high resolution information. The contrast of the lightest atoms tends to significantly decrease in the 80% blanking case but all atoms remain visible. Several artifacts are present in the images mainly due to the very long experimental acquisition time. The original image shows a clear drift, distorting the original lattice geometry. The presence of the stripes in the middle of the 50% blanking case are due to some sample instability during the acquisition and do not reflect any issues with the reconstruction algorithm.

In order to discriminate the beam blanker imperfections from reconstruction issues, we compared the reconstructed images with the reconstructions obtained from a virtually blanked image obtained by applying a digital mask on the unblanked experimental HAADF image as was typically done in papers discussing compressed sensing so far.[13,14,19] The results are shown in Figures 3(d) and 4(d).

In the case of the cross grating sample, simulated and experimental images look very similar, with the small image features being completely lost in the most sparsely sampled case. One could either incriminate the reconstruction algorithm, which may fail to sufficiently exploit the sparsity in the observed object. It could also be that the discrete cosine transform of the object itself is not sparse enough to be accurately represented by the chosen random sampling over the small image size acquired here. For the HRSTEM case, the difference between the virtually blanked images and the experimental ones is quite significant, pointing towards beam blanker artifacts. For the virtually blanked images, in both the 50% and 80% blanked cases, the reconstructions are approaching the fully sampled image quite closely with the only noticeable difference being a slight contrast reduction at sparser sampling. However, the experimentally blanked image reconstructions suffer from many more artifacts, going from a strong loss of contrast to losing the light atoms all together. These artifacts can have many origins, including remaining synchronization and timing issues, sample drift caused by increased exposure times, local sample charging issues affecting probe positioning, and possibly others. As sample drift and temporal instabilities of the instrument are related to the total acquisition time, they will disappear when the setup is changed to exploit the full beam blanker speed as the workaround with the ZL spectral acquisition is removed. Some of the mentioned artifacts could be overcome by using an electrostatic blanked even though this implementation will likely have its own artifacts.[26]

In this paper, we demonstrate the implementation of compressed sensing in a STEM making use of a fast electromagnetic beam blanker. Using a small solenoid placed in the condenser system of the microscope, the beam can be independently deflected for every pixel during a STEM image acquisition. The reconstruction of the images from the experimentally obtained sparsely sampled images shows that compressed sensing works significantly better for high resolution images, as compared to more irregular images as demonstrated with a cross grating sample. This is entirely expected as the discrete cosine transform of the high resolution images is significantly sparser in comparison to the one of the cross grating sample. At the atomic scale, artifacts induced by sample drift significantly alter the result, but can be overcome in the future when lower dwell times are used. The speed of the present setup remains insufficient for realistic use on beam sensitive samples but this limitation is imposed by technological factors which will be overcome in the near future. By overcoming these remaining technological challenges, a reduction of dose of at least 5 times can be expected depending on the type and sampling of the object. The implemented solution could potentially allow low dose imaging in STEM, improving the amount of information for life science applications which were not accessible before. In that sense, compressed sensing STEM could offer a cost effective alternative to, for example, direct electron detection cameras. Application in 3D tomographic acquisitions seem also particularly attractive as redundancy between different projections could be exploited. This would be especially important in the case of analytical 3D experiments.

A.B. and J.V. acknowledge funding from the European Research Council under the 7th Framework Program (FP7), ERC Starting Grant No. 278510 VORTEX and under a contract for an Integrated Infrastructure Initiative (Reference No. 312483 ESTEEM2), from the GOA Project SOLARPAINT and the POC Project I13/009 from the University of Antwerp. B.G. acknowledges the Research Foundation Flanders (FWO Vlaanderen) for a postdoctoral research grant. The QuAnTem microscope was partially funded by the Hercules Foundation. We thank Zhaoliang Liao from the Mesa+ laboratory at the University of Twente for the perovskite test sample.

[1]H. Rose, "Criteria and prospects for realizing optimum electron microscopes," Microsc. Microanal. **13**(Supplement S02), 134–135 (2007).
[2]D. A. Muller, "Structure and bonding at the atomic scale by scanning transmission electron microscopy," Nat. Mater. **8**(4), 263–270 (2009).
[3]U. Kaiser, J. Biskupek, J. C. Meyer, J. Leschner, L. Lechner, H. Rose, M. Stöger-Pollach, A. N. Khlobystov, P. Hartel, H. Müller, M. Haider, S. Eyhusen, and G. Benner, "Transmission electron microscopy at 20 kV for imaging and spectroscopy," Ultramicroscopy **111**(8), 1239–1246 (2011).
[4]A.-C. Milazzo, A. Cheng, A. Moeller, D. Lyumkis, E. Jacovetty, J. Polukas, M. H. Ellisman, N.-H. Xuong, B. Carragher, and C. S. Potter, "Initial evaluation of a direct detection device detector for single particle cryo-electron microscopy," J. Struct. Biol. **176**(3), 404–408 (2011).
[5]B. E. Bammes, R. H. Rochat, J. Jakana, D.-H. Chen, and W. Chiu, "Direct electron detection yields cryo-EM reconstructions at resolutions beyond 3/4 Nyquist frequency," J. Struct. Biol. **177**(3), 589–601 (2012).
[6]X. Li, P. Mooney, S. Zheng, C. R. Booth, M. B. Braunfeld, S. Gubbens, D. A. Agard, and Y. Cheng, "Electron counting and beam-induced motion correction enable near-atomic-resolution single-particle cryo-EM," Nat. Methods **10**(6), 584–590 (2013).
[7]G. McMullan, A. R. Faruqi, D. Clare, and R. Henderson, "Comparison of optimal performance at 300 keV of three direct electron detectors for use in low dose electron microscopy," Ultramicroscopy **147**, 156–163 (2014).
[8]T. LaGrange, M. R. Armstrong, K. Boyden, C. G. Brown, G. H. Campbell, J. D. Colvin, W. J. DeHope, A. M. Frank, D. J. Gibson, F. V. Hartemann, J. S. Kim, W. E. King, B. J. Pyke, B. W. Reed, M. D. Shirk, R. M. Shuttlesworth, B. C. Stuart, B. R. Torralva, and N. D. Browning, "Single-shot dynamic transmission electron microscopy," Appl. Phys. Lett. **89**(4), 044105 (2006).
[9]M. Aidelsburger, F. O. Kirchner, F. Krausz, and P. Baum, "Single-electron pulses for ultrafast diffraction," Proc. Natl. Acad. Sci. **107**(46), 19714–19719 (2010).
[10]P. E. Batson, "Unlocking the time resolved nature of electron microscopy," Proc. Natl. Acad. Sci. **108**(8), 3099–3100 (2011).
[11]P. Binev, W. Dahmen, R. DeVore, P. Lamby, D. Savu, and R. Sharpley, "Compressed sensing and electron microscopy," in *Modeling Nanoscale Imaging in Electron Microscopy*, Nanostructure Science and Technology, edited by T. Vogt, W. Dahmen, and P. Binev (Springer, US, 2012), pp. 73–126.

[12]A. Stevens, H. Yang, L. Carin, I. Arslan, and N. D. Browning, "The potential for Bayesian compressive sensing to significantly reduce electron dose in high-resolution STEM images," Microscopy **63**(1), 41–51 (2014).
[13]M. Li, Z. Fan, H. Ji, and Z. Shen, "Wavelet frame based algorithm for 3d reconstruction in electron microscopy," SIAM J. Sci. Comput. **36**(1), B45–B69 (2014).
[14]Z. Saghi, M. Benning, R. Leary, M. Macias-Montero, A. Borras, and P. A. Midgley, "Reduced-dose and high-speed acquisition strategies for multi-dimensional electron microscopy," Adv. Struct. Chem. Imaging **1**(1), 1–10 (2015).
[15]E. J. Candès, J. K. Romberg, and T. Tao, "Stable signal recovery from incomplete and inaccurate measurements," Commun. Pure Appl. Math. **59**(8), 1207–1223 (2006).
[16]D. L. Donoho, "Compressed sensing," IEEE Trans. Inf. Theory **52**(4), 1289–1306 (2006).
[17]E. J. Candes and M. B. Wakin, "An introduction to compressive sampling," IEEE Signal Process. Mag. **25**(2), 21–30 (2008).
[18]S. K. Park and K. W. Miller, "Random number generators: Good ones are hard to find," Commun. ACM **31**(10), 1192–1201 (1988).
[19]H. S. Anderson, J. Ilic-Helms, B. Rohrer, J. Wheeler, and K. Larson, "Sparse imaging for fast electron microscopy," Proc. SPIE **8657**, 86570C–86570C–12 (2013).
[20]R. G. Medhurst, "HF resistance and self capacitance of single layer solenoids—Part 1," Wireless Eng. **24**, 35–43 (1947).
[21]R. G. Medhurst, "HF resistance and self capacitance of single layer solenoids—Part 2," Wireless Eng. **24**, 80–92 (1947).
[22]See https://www.arduino.cc/ for Arduino project.
[23]E. van den Berg and M. Friedlander, "Probing the Pareto frontier for basis pursuit solutions," SIAM J. Sci. Comput. **31**(2), 890–912 (2008).
[24]SPGL1: A solver for large-scale sparse reconstruction.
[25]Z. Liao, M. Huijben, Z. Zhong, N. Gauquelin, S. Macke, R. J. Green, S. Van Aert, J. Verbeeck, G. Van Tendeloo, K. Held, G. A. Sawatzky, G. Koster, and G. Rijnders, "Controlled lateral anisotropy in correlated manganite heterostructures by oxygen octahedral coupling," Nat. Mater. (to be published).
[26]Q. Ramasse, private communication (2015).